

Defined Substrates for Human Embryonic Stem Cell Growth Identified from Surface Arrays

Ratmir Derda[†], Lingyin Li[†], Brendan P. Orner^{*,†}, Rachel L. Lewis[§], James A. Thomson[§], and Laura L. Kiessling^{†,*,*}

[†]Department of Chemistry, 1101 University Avenue, University of Wisconsin–Madison, Madison, Wisconsin 53706,

^{*}Department of Biochemistry, 433 Babcock Drive, University of Wisconsin–Madison, Madison, Wisconsin 53706, and

[§]Department of Anatomy, 425 Henry Mall, Genome Center of Wisconsin, Madison, Wisconsin 53706. [†]Present address: Division of Chemistry and Biological Chemistry, School of Physical and Mathematical Sciences, Nanyang Technological University, 1 Nanyang Walk, Blk 5 Level 3, Singapore 637616

Signals emanating from interactions at cell–cell and cell–substrate interfaces complement those resulting from the binding of soluble factors; together, they create a niche to define cellular fate (1, 2). This interplay between soluble and immobilized factors appears to control the proliferation and differentiation of embryonic stem (ES) cells (3–6). Despite advances in our understanding of human ES cells (7–9), the signals that promote human ES cell self-renewal are unknown. As a result, a major challenge has been to develop defined conditions for culturing human ES cells. The cells can be propagated in a co-culture with mouse embryonic fibroblasts (MEFs) (10). Feeder-free culture conditions also exist; however, they typically involve adhesive substrates of poorly defined composition or extracellular matrix proteins purified from animal or human sources (6, 11–14). For human therapies, an important objective is to develop defined and reproducible conditions for culturing human ES cells that limit their exposure to animal-derived components (15). The development of stem-cell-based regenerative medicine and the creation of therapeutically viable ES cell lines, therefore, hinge on establishing defined culture conditions that promote stem cell self-renewal (12, 16, 17). We reasoned that multicomponent arrays could be used to discover cell–substrate interactions with the requisite properties.

Developing an array strategy to expedite the identification of conditions for human ES cell growth is challenging. Cell arrays have been used to capture populations of differentiated cells (18–21). Because their

ABSTRACT Methods for the rapid identification of defined cell growth conditions are lacking. This deficiency is a major barrier to the investigation and application of human embryonic stem (ES) cells. To address this problem, we developed a method for generating arrays of self-assembled monolayers (SAMs) in which each element constitutes a defined surface. By screening surface arrays, we identified peptidic surfaces that support ES cell growth and self-renewal. The ability of the active surface array elements to support ES cell growth depends on their composition: both the density of the peptide presented and its sequence are critical. These findings support a role for specific surface–cell interactions. Moreover, the data from the surface arrays are portable. They can be used to design an effective 3D synthetic scaffold that supports the growth of undifferentiated human ES cells. Our results demonstrate that synthetic substrates for promoting and probing human ES cell self-renewal can be discovered through SAM surface arrays.

*Corresponding author,
kiessling@chem.wisc.edu.

Received for review February 11, 2007
and accepted April 17, 2007.

Published online May 4, 2007
10.1021/cb700032u CCC: \$37.00

© 2007 by American Chemical Society

potential has not been diminished, ES cells, however, will be prone to undergo uncontrolled changes in response to environmental cues. To obtain reproducible results, we sought to design an array in which the elements differ in the ligands presented, not in topology, elasticity, or other bulk properties. With such a surface array, we anticipated that array elements that afford the desired responses could be used in different contexts. For example, they could be used to elucidate the target receptors or to design new materials that control cell behavior.

To generate array elements with the aforementioned properties, we planned to employ self-assembled monolayers (SAMs) of alkanethiols (ATs) on gold. ATs form reproducible and well-ordered surfaces (22–25). They can be patterned to generate array elements of any size and shape; specific and nonspecific interactions of cells with SAMs can be modulated simply by changing the chemical structure of the constituent AT. To obtain reproducible results with human ES cells, we wanted to present array elements that could allow for extended (>5 d) cell proliferation. To address this issue, we presented peptides, which are expected to be more stable than proteins (20, 26). Protein function can often be achieved with shorter peptide fragments: peptide sequences are known that interact with adhesion (27) and signaling receptors (28–31). Finally, we incorporated into our array design the understanding that cells often interact with extracellular ligands *via* multivalent binding (32); therefore, we generated our arrays using a strategy that allows binding epitope density to be varied. With these design criteria in mind, we set out to synthesize SAM arrays.

RESULTS AND DISCUSSION

Fabrication of the Array for Human ES Cell

Screening. The properties of human ES cells offer challenges for the design of surface arrays. Specifically, human ES cells do not clone efficiently; thus, they cannot be plated at low densities (6, 10, 12, 33). To obtain reliable data from the screens, the array element size must allow for multiple population doublings. By evaluating the behavior of human ES cells in culture, we concluded that the array elements should be at least 500 μm in length and width (Supplementary Figure 1). With array elements of this size, hundreds of different conditions can be screened in one square inch. We anticipate that the assay throughput will be increased (*i.e.*, array ele-

ment size decreased), as the limitations of current human ES cell culture conditions are overcome (34).

To compare ES cell proliferation on different array elements, each array element must have the same size and shape. High-throughput robotic spotting is generally employed for rapid fabrication of multicomponent arrays. Application of this method, however, affords circular array elements whose size is governed by interplay of liquid surface tension and surface adhesion. In such a procedure, array element size will vary if different solvents are used in fabrication. To avoid this limitation, we developed a two-step fabrication strategy. First, the array element size and shape are defined by photolithography. Second, robotic or manual spotting delivers the SAM precursors to each element surrounded by solvent-repellent background to generate the appropriate SAM array element. Perfluorinated ATs eschew interactions with typical organic and aqueous solvents; therefore, they bead common solvents. We reasoned that solutions containing peptide-presenting ATs could be spotted onto a perfluorinated surface patterned *via* photolithography to create a surface array (Figure 1, panels a and b) (35). As expected, this methodology is relatively insensitive to both volume and type of solvent (Supplementary Figure 2, panels a and b). Additionally, positional errors in spotting are corrected by the solvent-repelling properties of the background (Supplementary Figure 2, panel c) (36). The resistance of the fabrication method to spotting errors allows rapid and reproducible fabrication of arrays with a large number of array elements of any size and shape. Importantly, SAMs derived from perfluorinated ATs resist nonspecific cell adhesion; therefore, they can serve as an appropriate background in subsequent cell-based assays (Figure 1, panel c) (37, 38).

Screening Arrays That Present Peptide Ligands. Biological substrates that allow for human ES cell self-renewal guided the design of our surface arrays. Specifically, in the protein mixtures typically employed as substrates for human ES cell growth, the major constituent is the extracellular matrix protein laminin (6, 12–14). A number of laminin-derived peptides have been shown to support adhesion of primary cells and immortalized cell lines, and laminin peptides have been shown to interact with proteins that signal (*e.g.*, integrins). We therefore reasoned that biologically active peptides derived from laminin might promote ES cell growth. To test this hypothesis, we generated arrays that

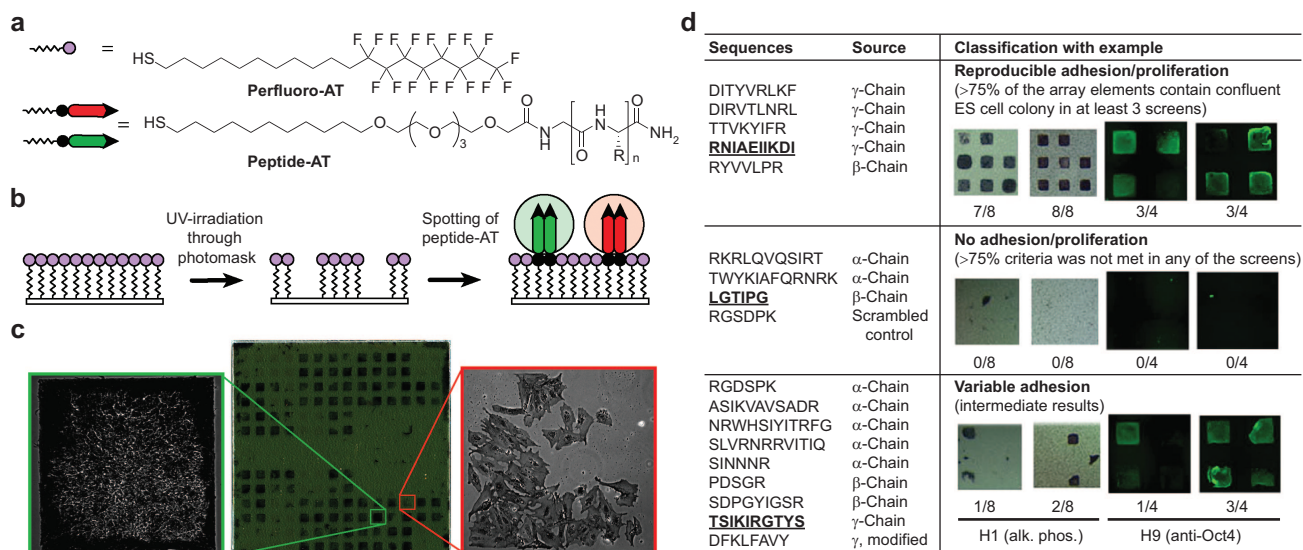


Figure 1. Surface array screen for ES cell growth and self-renewal. **a)** Structure of alkanethiols used for the assembly of the array. “R” denotes amino acid side chains. **b)** A two-step process was employed to generate the arrays. A uniform SAM composed of perfluoro-AT was photopatterned, and solutions of peptide-ATs were spotted onto the exposed gold areas to form peptide-terminated SAM array elements. **c)** A representative array containing 18 different peptide-ATs was screened to identify surfaces that promote proliferation of ES cell line H9. The peptide-displaying SAMs are arranged in a mirror-symmetric pattern (bottom and top halves of chip have identical array elements). Each half of the array contains 18 laminin-derived peptide-ATs spotted in groups of four (2×2 elements) arranged in a left-to-right horizontal comb pattern. The remaining array elements are filled with nonadhesive glucamine-AT (35, 54) (see Supplementary Figure 3 for a map of the layout). The array was incubated with media containing 20% FBS and thoroughly washed with serum-free media. Cells were grown on the array for 6 d in CM, fixed, and stained for alkaline phosphatase (AP). The positions of cell growth are symmetric and emphasize the reproducibility of ES cell responses to the array elements. The array was mounted onto a glass slide and scanned using a flatbed scanner. The phase-contrast $10\times$ images reveal morphological differences between AP-positive undifferentiated (left) and AP-negative differentiated ES cells (right). Array dimensions: 22×22 mm; each element is 0.8 mm. **d)** Summary of results from multiple screens for 18 laminin-derived peptides and ES cell lines H1 and H9. Laminin chain origin is shown for each peptide. Following 5–7 d of growth, substrates were categorized according to their ability to accommodate confluent (square-shaped) and undifferentiated colonies, as judged by staining for alkaline phosphatase (purple) or Oct4 (green). Each synthetic substrate was tested four to eight times in each screen; therefore, the fraction of array elements presenting square ES cell colonies serves as a convenient measure of substrate efficiency. Representative results for one peptide in each category are shown, and the corresponding peptide sequences are underlined. The apparent higher intensity of Oct4 around the edges of the array element can be attributed to differences in thicknesses of ES cell colony around the edges (41) or differentiation of overcrowded cells in the middle of the array element. The latter is not observed when cells are cultured on large area substrates that do not restrict colony growth (Figure 2).

present laminin-derived peptides at uniform density and with a defined peptide orientation (Figure 1, panel b).

An array containing 18 different laminin-derived peptides was screened to identify those surfaces that support the proliferation and self-renewal of two human ES cell lines (H1 and H9) (Figure 1, panels c and d). In each screening experiment, the surface array was exposed to a suspension of human ES cells. Cell attachment and growth on the array in the presence of media conditioned by MEFs was allowed to proceed for 5–7 d. The cells were fixed and stained for visualization and evalu-

ation of their state using markers of ES cell pluripotency. Specifically, we tested for the presence of endogenous alkaline phosphatase and octamer-binding transcription factor 4 (Oct4). Pluripotent human ES cells produce these proteins, but their production is down-regulated upon differentiation (10). When alkaline phosphatase activity was visualized using a chromogenic substrate those array elements that support ES cell proliferation could be readily identified by visual inspection (Figure 1, panel c). Each element was evaluated for activity in replicates of 4–8 within a chip; to ensure the reproducibility of results, we also compared

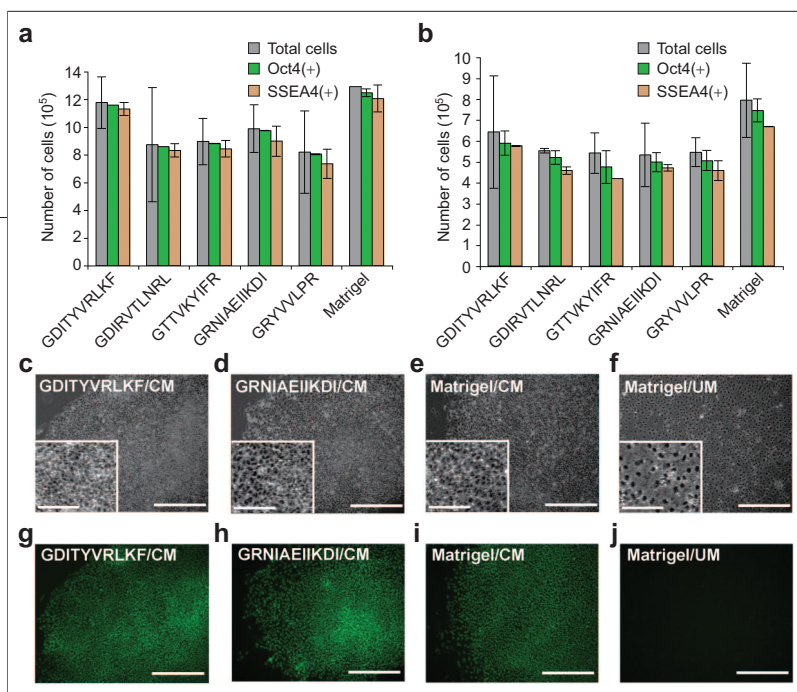


Figure 2. Proliferation efficiency and production of markers of pluripotency for human ES cell lines H1 (a) and H9 (b) grown on synthetic SAM substrates are similar to those grown on Matrigel. The graphs summarize the results from two independent experiments. The number of Oct4 and SSEA4 (+) cells is a product of averaged cell count and averaged percentage of Oct4 and SSEA4 positive cells obtained. Error bars represent 1 standard deviation between two flow cytometry experiments and do not include the standard deviation of cell counting. Cells proliferated on SAM substrates for 6 d display morphology (c, d) and level of Oct4 expression (g, h) similar to those of undifferentiated ES cells on Matrigel/CM (e, i). As a control, ES cells were proliferated on Matrigel in unconditioned medium (UM), which contains 20% defined FBS to induce differentiation. The morphology (see higher magnification insets) of the differentiated cells (f) is different from that of ES cells (c, d, e). Additionally, differentiated cells give rise to little to no Oct4 staining (j). Images were obtained with an epifluorescence microscope using an identical acquisition time for each image. For each of the four images depicted, the brightness and contrast were adjusted simultaneously. Scale bar = 0.2 mm. Inset scale bar = 60 μm .

the activity of array elements between independently fabricated chips and different ES cell lines.

Our surfaces were biased to present array elements that could support cell adhesion, as we reasoned ES cell adhesion would be critical for self-renewal. In support of this hypothesis, several of the array elements we selected had some level of activity. We used a combination of growth efficiency and staining for markers of pluripotency to identify the most efficient substrates supporting proliferation of undifferentiated ES cells. Each array element had uniform size and square shape; therefore, array elements containing square-shaped colonies of ES cells staining positive for a marker of pluripotency were easily identified as “hits”. Every substrate was tested in replicates in every array. Thus, for every substrate, the ratio of the array element presenting “square colonies” to the total number of peptide-displaying elements served as a simple measure of substrate efficiency (Figure 1, panel d, and Supplementary Figure 3). Of the 18 screened peptide sequences that exhibit activity in cell adhesion assays, 5 were effective at

promoting ES cell proliferation in an undifferentiated state (Figure 1, panel d). We focused on these array elements because of their potential for yielding defined conditions for ES cell self-renewal.

Human ES Cells Cultured on Peptidic Substrates Remain Undifferentiated.

It was critical to determine whether the substrates yielding robust positive outcomes in our screens would give rise to uniform populations of undifferentiated cells. Although surfaces that support ES cell growth can be identified by staining the arrays for ES cell pluripotency, this analysis provides a semiquantitative measure. The intensity depends on the number of cells within the array element that stain positive for the marker; cells that do not stain are not detected. Moreover, staining intensity can be influenced by cell proliferation rates. Dual-color microscopy analysis (e.g., 4',6-diamidino-2-phenylindole (DAPI) and Oct4 stain) can resolve these problems for array elements with a small number of cells. We employed flow cytometry as a means to evaluate individual cells within a large population.

To generate a sizable population (10^5 – 10^6 cells), we cultivated human ES cells on gold-coated glass slides (22×22 mm) containing a SAM presenting a single peptide sequence. The resulting cells were analyzed for the presence of the transcription factor Oct4 and the cell surface marker stage-specific embryonic antigen-4 (SSEA4), both of which are produced by undifferentiated human ES cells (10). We evaluated ES cells that had been cultured on Matrigel for comparison (13). The synthetic surfaces are as effective as Matrigel at supporting cell proliferation (Figure 2, panels a and b). They also appear to maintain cells in the undifferentiated state: the percentages of cells proliferated on the synthetic surface that test positive for both ES cell markers are similar to those of cells growing on Matrigel (96–99% for Oct4 and 84–90% for SSEA4). To confirm that our analysis can detect ES cell differentiation, we proliferated cells in unconditioned growth medium containing fetal bovine serum (FBS) (6). After 6 d, we analyzed the cells by flow cytometry and found that the level of Oct4 expression decreased to $\sim 20\%$ (Supplementary Table 1). Additionally, microscopy analysis indicates that the cells proliferating under conditions known to induce differentiation have a different morphology (compare Figure 2, panels c–e and f) and level of Oct4 expression (compare Figure 2, pan-

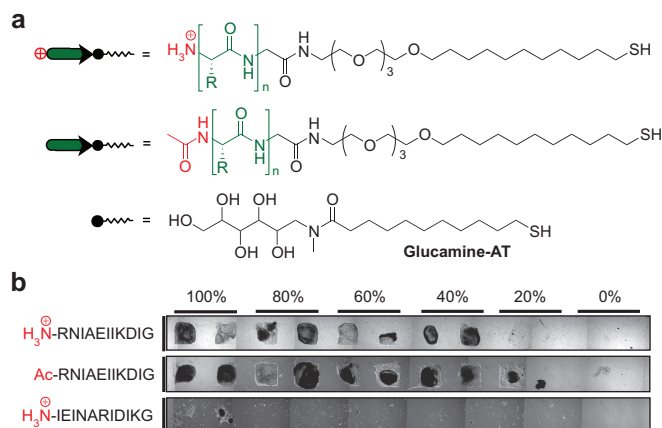


Figure 3. Testing the specificity of the identified peptide epitopes in array format. **a)** Peptide-ATs can be synthesized with either a free or acetylated N-terminus to control the net charge of the peptide-AT and, therefore, the overall surface charge density of the resultant SAM. The peptide surface density and charge surface density can be tuned independently by forming mixed monolayers of differently charged peptide-AT with glucamine-AT (35, 54), an AT that exhibits no cell binding. **b)** Results from varying the charge, peptide density, and peptide sequence to assess the specificity of interactions. The array was fabricated by spotting solutions containing mixtures of corresponding AT-peptide with a glucamine-AT. The percentages are the mole fractions of the active peptide-AT included in the spotted mixture. Depicted is a mosaic phase-contrast image of live human ES cell line H1 after 7 d of proliferation. The size of each array element is 0.8×0.8 mm.

els g–i and j) than those of undifferentiated ES cells. These findings indicate that our array strategy can yield synthetic, defined surfaces appropriate for proliferation of undifferentiated human ES cells.

Evaluation of the Specificity of the Identified

Substrates. Our surface array was designed not only to discover surfaces that give rise to desired cellular responses but also to identify the receptors responsible (35). If the peptide ligands presented by the surface act via a specific receptor, their ability to support ES cell proliferation should depend on the specific sequence displayed. In probing the selectivity of the interactions, we examined an active peptide from our screen, RNIAEIKDI. Although the receptor has not been identified, this sequence had been shown previously to promote neurite extension (39, 40). Because cells can adhere to charged surfaces, we tested whether the net charge (+1) of this peptide is important for the activity of the resulting surface. When the peptide N-terminus is acetylated (Ac-RNIAEIKDI), there is no net charge (Figure 3, panel a). SAMs presenting either RNIAEIKDI or Ac-RNIAEIKDI at

various surface densities exhibit similar activities (Figure 3, panel b). This result suggests that the ability of the ES cells to proliferate on these surfaces is not due to charge-dependent nonspecific adhesion. Stronger support for the importance of the specific peptide sequence comes from analysis of a surface displaying a scrambled sequence: no detectable cell adhesion occurs at surface densities <100% (Figure 3, panel b, bottom row). Thus, the peptide sequence presented is critical for the ability of the array element to support cell growth. These results indicate that specific interactions critical for cell proliferation can be imparted by array elements.

Our data suggest that the ES cell–substrate interaction results from receptor–ligand interactions. The data (Figure 3, panel b) also indicate that the ligand must be presented at relatively high density on the surface to support human ES cell proliferation. This finding is consistent with the need for human ES cells to adhere to an array element with sufficient avidity and in sufficient density

to give rise to a viable colony. We surmise that the need for a relatively high density presentation of ligands stems from a low concentration of the target receptor on the cell surface.

To illuminate how the ligand density on a surface and cell surface receptor concentrations influence cell adhesion, we tested the binding of cell lines that display different levels of target receptors (α_v integrins) to surfaces substituted with different levels of RGD peptides (Supplementary Figure 4). Using a battery of five cell lines that display different levels of the integrin receptor, we found those with low receptor levels adhere only to surfaces with a high ligand density. Our results are in accord with the preference of ES cells for biomaterials presenting a high density of RGD epitopes (41). In contrast, cell lines with a high level of receptors can adhere to surfaces presenting both high and low densities of specific ligands. Because the levels of receptors important for ES cell binding or self-renewal cannot be anticipated, our results indicate that it is beneficial to use surfaces substituted with a relatively high epitope density in

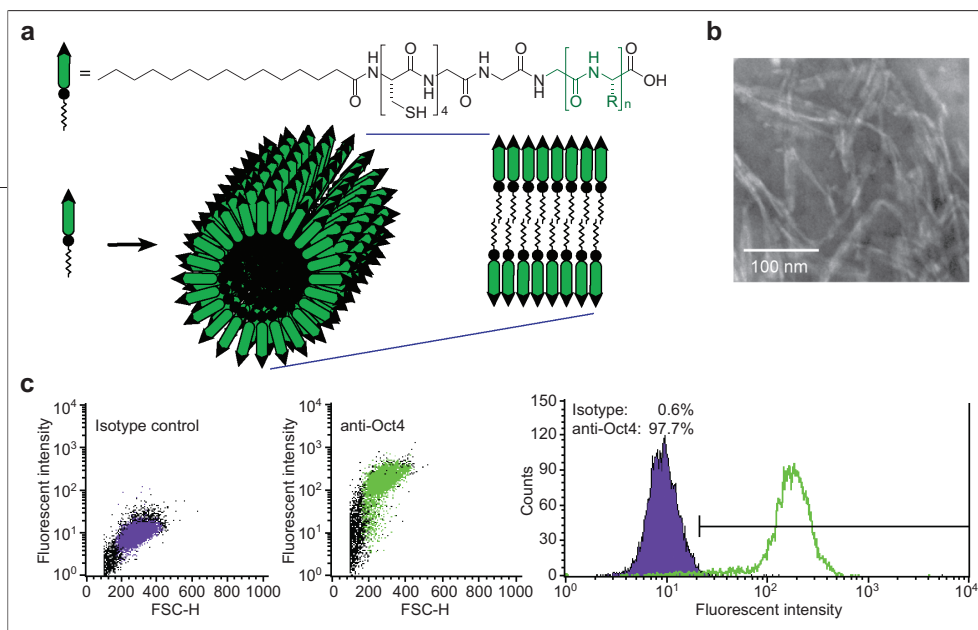


Figure 4. Assembly and utility of 3D substrates presenting identified peptides. a) The structure of the peptide amphiphile used for the hydrogel fabrication and the schematic illustration of the assembly of peptide amphiphiles into peptide-presenting nanofibers. A cross section of nanofiber is shown to illustrate the similarity of ligand presentation to that in SAMs. b) TEM data confirming nanofiber morphology for gel formed from the peptide–amphiphile containing RNIAEIIKDI sequence. c) Oct4 flow cytometry analysis of human ES cell line H9 proliferated for 4 d on RNIAEIIKDI-presenting hydrogel. The Oct4 histogram is characteristic of undifferentiated ES cells (Supplementary Table 1, panel d).

preliminary screens. With this approach, ligands that interact with either high- or low-abundance receptors can be identified. Moreover, our data suggest that the receptor for RNIAEIIKDI is present only at a low level.

In the course of long-term interactions of cells and growth substrates, extensive remodeling of the substrates by cells occurs. Although we have demonstrated that the peptide sequence is important for human ES cell interaction with the synthetic surface, we cannot eliminate contributions from adsorption of ES-cell-secreted proteins or proteins from the growth media. Dissecting the role of surface-sequestered proteins in ES cell growth on complex substrates (*e.g.*, a MEF feeder layer (10) or Matrigel (13)) is a challenge because of their inherent complexity. Because SAMs are chemically defined, they can provide a platform for the identification of surface-captured proteins that promote desirable cellular responses.

Portability of the Information from the Screen:

Fabrication of Biomaterials. Because ES cell proliferation depends on the peptide sequence presented by the array element, we reasoned that the peptide sequences identified should be portable; they should function as recognition elements in other contexts. One application for such sequences is in the design of biomaterials that could serve as substrates for the growth of human ES cells (24, 41–46). We reasoned that a tailored hydrogel could provide an attractive and convenient alternative to SAMs. Moreover, the benefits

of 3D over 2D matrices for culturing cells are often substantial (47–49).

In our design of a 3D scaffold, we were guided by the data from our array. Specifically, our experiments suggested that a high-density presentation of the active peptide sequence RNIAEIIKDI might prove effective. Stupp and co-workers (50) had shown that amphiphiles possessing alkyl and peptide groups form nanofibers. Like SAMs, these cylindrical nanofibers present ligands at a high density: they display $\sim 7 \times 10^{14}$ epitopes/

cm^2 with a single, defined orientation (Figure 4, panel a) (51, 52). Thus, we hypothesized that the resultant hydrogel would mimic the display of peptides identified using SAM arrays and, therefore, support ES cell growth. To test this hypothesis, we synthesized the amphiphile containing the RNIAEIIKDI sequence. After exposure to conditions that lead to assembly and gel formation, transmission electron microscopy (TEM) confirmed that the resulting material was composed of nanofibers (Figure 4, panel b). This material supports the adhesion and proliferation of ES cells. Moreover, the cells growing in its presence remain undifferentiated, as judged by flow cytometry analysis using an anti-Oct4 antibody (Figure 4, panel c). These cells also exhibit normal ES cell morphology; they are tightly packed with a high nucleus-to-cytoplasm ratio (Supplementary Figure 5). These results demonstrate that the specific epitopes identified using surface arrays can serve as recognition elements in different contexts. Thus, a major benefit of our surface arrays is their ability to provide an avenue for the design of biomaterials that support ES cell self-renewal.

Our results indicate that SAM arrays can facilitate the discovery of appropriate substrates for human ES cell growth. A distinguishing feature of these arrays is their ability to afford recognition elements that function in different contexts. The portability of these recognition elements suggests that they can be used to identify receptor–ligand pairs critical for stem cell self-renewal. Thus, SAM arrays offer a rich and flexible

foundation for the high-throughput identification of surfaces that support ES cell growth. We note that such arrays could also be used to explore how surface interactions influence cell migration, prolifera-

tion, and differentiation. All of these are processes valuable for cell-based therapeutics. The approach we have outlined can therefore be used to facilitate advances in regenerative medicine.

MATERIALS AND METHODS

Reagent Synthesis. Peptide-ATs were synthesized using reported procedures (35, 53). Briefly, a peptide sequence of interest was assembled *via* automated peptide synthesizer (Pioneer, PerSeptive Biosystems) using a PAL-polystyrene resin (Applied Biosystems) and standard Fmoc chemistry. The identity of the synthesized peptide sequence was confirmed by cleaving the peptide from a small amount of resin and analyzing it by MALDI-TOF mass spectrometry (MS). To generate the peptide-ATs, a trityl-protected alkanethiol containing a carboxylic acid was conjugated to the free N-terminus of resin-bound peptides (35, 53). Cleavage of peptide-ATs from the resin and side-chain protecting group removal was carried out in 92.5% trifluoroacetic acid, 2.5% H₂O, 2.5% triisopropylsilane, and 2.5% ethanedithiol for 2 h. The resulting material was purified by HPLC. The identity and purity of each AT-peptide were confirmed using LC/MS. Supplementary Table 2 depicts LC/MS traces of representative AT-peptides.

The peptide amphiphile for the hydrogel formation was synthesized using a procedure similar to that reported (50). Briefly, the peptide sequence CCCC GGGRNIAEIIKDI was synthesized using an automated peptide synthesizer and Fmoc chemistry starting from preloaded Fmoc-L-Ile-PEG-PS resin (Applied Biosystems). Following Fmoc removal from the final residue, pentadecanoic acid (Aldrich) was conjugated to the free N-terminus. Peptide cleavage from resin was performed as described above. The peptide was precipitated three times from ether and lyophilized to yield the peptide-amphiphile as white flakes. The amphiphile was characterized by LC/MS (Supplementary Table 2) and high-resolution MS (electrospray ionization) to afford 1007.5057, which corresponds to [MHN₂]²⁺ (calculated for C₈₅H₁₅₁N₂₂O₂₄S₄Na = 1007.5026). The hydrogel was assembled directly in the wells of a 6- or 12-well plate from a 1% aqueous solution of the peptide-amphiphile. Filter paper soaked in concentrated HCl was attached to the plate lid, and the plate was closed for 20–40 min to allow slow diffusion of HCl vapor into the amphiphile solution. The assembled gel was treated with saturated aqueous iodine solution for 20 min and gently washed with ethanol to eliminate the traces of iodine (repetitive washes were conducted until no color was observed). All subsequent manipulations were done in the laminar-flow hood with sterile reagents.

Array Fabrication. Gold-coated glass coverslips were purchased from EMF Corp. Gold surface was inspected by scanning electron microscopy and atomic force microscopy (Supplementary Figure 6). Coverslips were immersed in a 1 mM solution of perfluoro-AT in absolute ethanol. After >48 h, substrates were rinsed with ethanol and dried under a stream of nitrogen. The resultant perfluorinated SAMs were characterized *via* contact angle goniometry (Supplementary Figure 6). Coverslips were irradiated with 1 kW 4×4 beam Deep UV Illuminator (Spectra-Physics) through a quartz photomask (Photo Sciences) for 2 h. Irradiated samples were rinsed thoroughly with ethanol and dried under a stream of nitrogen. Spotting of AT solutions onto the bare gold areas was performed within 2 h of the photolithography. Solutions of peptide-ATs (or glucamine-AT) (1 mM) in 1:10 (v/v) DMF/water were used to fabricate arrays outlined in Figure 1 and Supplementary Figure 3. Solutions of peptide-AT

and glucamine-AT (1 mM) in 1:10 (v/v) DMF/water were mixed in 4:1, 3:2, 2:3 and 1:4 (v/v) ratio, and these solutions were used to fabricate the mixed SAMs in the arrays outlined in Figure 3. Spotting was performed manually using a P2-Pipetman in a generic humidity chamber. Spotted arrays were stored in the humidity chamber for 12 h and washed repeatedly with ethanol and water. Arrays placed in wells of a six-well plate (Nunc), sterilized by brief incubation with 70% ethanol, and dried under UV light for 1 h in a laminar-flow hood.

Cell Culture. Human ES cell lines, H1 and H9, were grown on Matrigel-coated plates using MEF conditioned media (CM) supplemented with 4 ng/mL bFGF (Invitrogen). To produce CM, MEFs were seeded at a density of 2.12×10^5 cells/mL and grown using medium consisting of Dulbecco's modified Eagle's medium with F-12 nutrition supplement (DF-12), 20% Knockout serum replacement, 2 mM L-glutamine, 1% nonessential amino acids (Invitrogen), and 0.1 mM β-mercaptoethanol (Aldrich). Both cell lines (ES and MEF) were maintained at 37 °C/5% CO₂ with CM collected and cells fed approximately every 24 h. Cell suspensions were made by treating with dispase (2 mg/mL) for 5–6 min. The cells were scraped from the surface and suspended in CM.

The arrays in six-well plates were incubated with DF-12 containing 20% defined FBS overnight at 36 °C and washed thoroughly with DF-12 (3 × 5 min). ES cell suspensions were plated in the well atop the chip (2.5 mL of media, $\sim(3-7) \times 10^5$ cells/chip) and allowed to adhere overnight. Media exchange to fresh CM (with removal of floating and nonadherent cells) was performed daily.

Hydrogel-coated wells were thoroughly washed with DF-12 to eliminate the traces of ethanol. To ensure the absence of any toxic agents in hydrogel, the hydrogel-coated wells were incubated with DF-12 + 20% FBS for 12 h and washed thoroughly with DF-12. ES cell suspensions were plated at $\sim(3-7) \times 10^5$ cells/well. Media exchange to fresh CM (with removal of floating and non-adherent cells) was performed daily for 5–6 d prior to analysis by flow cytometry.

Test for Alkaline Phosphatase Activity. After propagation of the ES cells, the media was removed from the wells containing the chips. The cells were fixed with 1% formaldehyde. Chips were stained using a BCIP/NBT substrate kit (Vector Labs) according to the manufacturer's procedure. The chips were washed with phosphate-buffered saline (PBS) and distilled water, dried in air, and permanently mounted using VectaMount (Vector Labs). Images of the whole array were obtained using a flatbed scanner or dissecting microscope with 1× objective and color CCD camera.

Cell Immunostaining with Oct4 Antibody. After propagation of the ES cells, the medium was removed from the wells. The cells were fixed with 3% formaldehyde for 10 min, permeabilized with 0.1% Triton-X in PBS for 20 min, and blocked with 5% non-fat milk and 0.1% Triton-X in PBS for 30 min. A 1:200 dilution of Oct4 antibody in 0.1% Triton-X in PBS was added, and the array with cells was incubated for 1 h at RT. Cells were washed two times with 0.1% Triton-X in PBS and incubated with 1:500 of goat-anti-mouse Alexa488-labeled IgG for 1 h at RT. Arrays were washed and mounted using VectaShield (Vector Labs) and imaged using an epifluorescent inverted microscope with a 5×-

objective using automated mosaic imaging (9 × 11 images per one array). Individual colonies growing on Matrigel or one-component SAMs (Figure 3) were imaged using an epifluorescence inverted microscope with 10× objective.

Flow Cytometry Analysis for Pluripotency Markers. After propagation of the ES cells, the medium was removed from the wells containing the SAM substrates or Matrigel control. Human ES cells were treated with the protease dispase (2 mg/mL, 5 min). The dispase-containing solution was removed. Adherent ES colonies were gently washed three times with DF-12 and detached by purging with media and scratching. Cells were further separated by treatment with 1× trypsin–EDTA solution for 5 min. Cells were fixed with aqueous 1% formaldehyde for 10 min at 36 °C. For Oct4 immunostaining, cells were permeabilized with ice-cold methanol for 30 min. Cells were treated with 100 μL of 1:100 solution of the Oct4-recognizing antibody (Santa Cruz) or mouse IgG isotype antibody in fluorescence activated cell sorting (FACS)/Triton buffer (10% FBS, 1% NaN₃, 0.1% Triton-X in PBS) overnight at 4 °C. Cells were washed in FACS/Triton buffer and treated with 100 μL of 1:400 dilution of rabbit–anti-mouse Alexa488-labeled antibody (Molecular Probes) for 1 h at RT.

For SSEA4 immunostaining nonpermeabilized cells were incubated with 100 μL of 1:100 dilution of SSEA4 antibody (Chemicon Intl.) or isotype IgG antibody in FACS buffer (10% FBS, 1% NaN₃ in PBS) overnight at 4 °C. Cells were washed in FACS buffer and stained with 100 μL of 1:400 dilution of rabbit–anti-mouse Alexa488-labeled antibody for 1 h at RT. The samples were analyzed using FACScalibur (Becton Dickinson) using 530/30 band pass filter. The percentage of Oct4-positive (SSEA4-positive) cells was assessed by comparing the cell number determined with Anti-Oct4 with that obtained using the corresponding isotype IgG antibody. The threshold was defined with respect to the cells from that same growth conditions stained with isotype IgG antibody. The threshold staining intensity was assigned to 1% of cell population in the isotype control population.

Acknowledgments: This research was supported by the Defense Advanced Research Projects Agency (N66001-03-1-8932), the National Institutes of Health (NIH) (AI055258), and the University of Wisconsin Materials Research Science and Engineering Center (DMR-0520527). We thank the W. M. Keck Foundation for supporting the Center for Chemical Genomics. B.P.O. was supported by a postdoctoral fellowship from the NIH (AG19550). We thank R. J. Massey and University of Wisconsin–Madison Medical School Electron Microscope Facility for help with TEM and acknowledge R. K. Noll and J. R. Jacobs (University of Wisconsin Materials Science Center) and K. Y. Tse (Department of Chemistry) for assistance with surface characterization. We thank G. L. Case for assistance with automated peptide synthesis.

Supporting Information Available: This material is available free of charge via the Internet.

REFERENCES

- Huang, S., and Ingber, D. E. (1999) The structural and mechanical complexity of cell-growth control, *Nat. Cell Biol.* **1**, E131–E138.
- Spradling, A., Drummond-Barbosa, D., and Kai, T. (2001) Stem cells find their niche, *Nature* **414**, 98–104.
- Beattie, G. M., Lopez, A. D., Bucay, N., Hinton, A., Firpo, M. T., King, C. C., and Hayek, A. (2005) Activin A maintains pluripotency of human embryonic stem cells in the absence of feeder layers, *Stem Cells* **23**, 489–495.
- James, D., Levine, A. J., Besser, D., and Hemmati-Brivanlou, A. (2005) TGF beta/activin/nodal signaling is necessary for the maintenance of pluripotency in human embryonic stem, *Development* **132**, 1273–1282.
- Kim, S. J., Cheon, S. H., Yoo, S. J., Kwon, J., Park, J. H., Kim, C. G., Rhee, K., You, S., Lee, J. Y., Roh, S. I., and Yoon, H. S. (2005) Contribution of the PI3K/Akt/PKB signal pathway to maintenance of self-renewal in human embryonic stem cells, *FEBS Lett.* **579**, 534–540.
- Xu, R. H., Peck, R. M., Li, D. S., Feng, X. Z., Ludwig, T., and Thomson, J. A. (2005) Basic FGF and suppression of BMP signaling sustain undifferentiated proliferation of human ES cells, *Nat. Methods* **2**, 185–190.
- Boyer, L. A., Lee, T. I., Cole, M. F., Johnstone, S. E., Levine, S. S., Zucker, J. R., Guenther, M. G., Kumar, R. M., Murray, H. L., Jenner, R. G., Gifford, D. K., Melton, D. A., Jaenisch, R., and Young, R. A. (2005) Core transcriptional regulatory circuitry in human embryonic stem cells, *Cell* **122**, 947–956.
- Lee, T. I., Jenner, R. G., Boyer, L. A., Guenther, M. G., Levine, S. S., Kumar, R. M., Chevalier, B., Johnstone, S. E., Cole, M. F., Isono, K., Kosaki, H., Fuchikami, T., Abe, K., Murray, H. L., Zucker, J. P., Yuan, B. B., Bell, G. W., Herbolsheimer, E., Hannett, N. M., Sun, K. M., Odom, D. T., Otte, A. P., Volkert, T. L., Bartel, D. P., Melton, D. A., Gifford, D. K., Jaenisch, R., and Young, R. A. (2006) Control of developmental regulators by polycomb in human embryonic stem cells, *Cell* **125**, 301–313.
- Sperger, J. M., Chen, X., Draper, J. S., Antosiewicz, J. E., Chon, C. H., Jones, S. B., Brooks, J. D., Andrews, P. W., Brown, P. O., and Thomson, J. A. (2003) Gene expression patterns in human embryonic stem cells and human pluripotent germ cell tumors, *Proc. Natl. Acad. Sci. U.S.A.* **100**, 13350–13355.
- Thomson, J. A., Itskovitz-Eldor, J., Shapiro, S. S., Waknitz, M. A., Swiergiel, J. J., Marshall, V. S., and Jones, J. M. (1998) Embryonic stem cell lines derived from human blastocysts, *Science* **282**, 1145–1147.
- Amit, M., Shariki, C., Margulets, V., and Itskovitz-Eldor, J. (2004) Feeder layer- and serum-free culture of human embryonic stem cells, *Biol. Reprod.* **70**, 837–845.
- Ludwig, T. E., Levenstein, M. E., Jones, J. M., Berggren, W. T., Mitchen, E. R., Frane, J. L., Crandall, L. J., Daigh, C. A., Conard, K. R., Piekarczyk, M. S., Llanas, R. A., and Thomson, J. A. (2006) Derivation of human embryonic stem cells in defined conditions, *Nat. Biotechnol.* **24**, 185–187.
- Xu, C., Inokuma, M. S., Denham, J., Golds, K., Kundu, P., Gold, J. D., and Carpenter, M. K. (2001) Feeder-free growth of undifferentiated human embryonic stem cells, *Nat. Biotechnol.* **19**, 971–974.
- Xu, C., Rosler, E., Jiang, J. J., Lebkowski, J. S., Gold, J. D., O'Sullivan, C., Delavan-Boorsma, K., Mok, M., Bronstein, A., and Carpenter, M. K. (2005) Basic fibroblast growth factor supports undifferentiated human embryonic stem cell growth without conditioned medium, *Stem Cells* **23**, 315–323.
- Martin, M. J., Muotri, A., Gage, F., and Varki, A. (2005) Human embryonic stem cells express an immunogenic nonhuman sialic acid, *Nat. Med.* **11**, 228–232.
- Lu, J., Hou, R. H., Booth, C. J., Yang, S. H., and Snyder, M. (2006) Defined culture conditions of human embryonic stem cells, *Proc. Natl. Acad. Sci. U.S.A.* **103**, 5688–5693.
- Yao, S., Chen, S., Clark, J., Hao, E., Beattie, G. M., Hayek, A., and Ding, S. (2006) Long-term self-renewal and directed differentiation of human embryonic stem cells in chemically defined conditions, *Proc. Natl. Acad. Sci. U.S.A.* **103**, 6907–6912.
- Anderson, D. G., Levenberg, S., and Langer, R. (2004) Nanoliter-scale synthesis of arrayed biomaterials and application to human embryonic stem cells, *Nat. Biotechnol.* **22**, 863–866.
- Chen, D. S., and Davis, M. M. (2006) Molecular and functional analysis using live cell microarrays, *Curr. Opin. Chem. Biol.* **10**, 28–34.
- Flaim, C. J., Chien, S., and Bhatia, S. N. (2005) An extracellular matrix microarray for probing cellular differentiation, *Nat. Methods* **2**, 119–125.
- Falconnet, D., Csucs, G., Grandin, H. M., and Textor, M. (2006) Surface engineering approaches to micropattern surfaces for cell-based assays, *Biomaterials* **27**, 3044–3063.

22. Love, J. C., Estroff, L. A., Kriebel, J. K., Nuzzo, R. G., and Whitesides, G. M. (2005) Self-assembled monolayers of thiolates on metals as a form of nanotechnology, *Chem. Rev.* **105**, 1103–1169.
23. Smith, R. K., Lewis, P. A., and Weiss, P. S. (2004) Patterning self-assembled monolayers, *Prog. Surf. Sci.* **75**, 1–68.
24. Castner, D. G., and Ratner, B. D. (2002) Biomedical surface science: Foundations to frontiers, *Surf. Sci.* **500**, 28–60.
25. Lopez, G. P., Albers, M. W., Schreiber, S. L., Carroll, R., Peralta, E., and Whitesides, G. M. (1993) Convenient methods for patterning the adhesion of mammalian-cells to surfaces using self-assembled monolayers of alkanethiolates on gold, *J. Am. Chem. Soc.* **115**, 5877–5878.
26. MacBeath, G., and Schreiber, S. L. (2000) Printing proteins as microarrays for high-throughput function determination, *Science* **289**, 1760–1763.
27. Plow, E. F., Haas, T. K., Zhang, L., Loftus, J., and Smith, J. W. (2000) Ligand binding to integrins, *J. Biol. Chem.* **275**, 21785–21788.
28. Anderson, A. A., Kendal, C. E., Garcia-Maya, M., Kenny, A. V., Morris-Triggs, S. A., Wu, T., Reynolds, R., Hohenester, E., and Saffell, J. L. (2005) A peptide from the first fibronectin domain of NCAM acts as an inverse agonist and stimulates FGF receptor activation, neurite outgrowth and survival, *J. Neurochem.* **95**, 570–583.
29. Kiselyov, V. V., Skladchikova, G., Hinsby, A. M., Jensen, P. H., Kula-hin, N., Soroka, V., Pedersen, N., Tsetlin, V., Poulsen, F. M., Berezin, V., and Bock, E. (2003) Structural basis for a direct interaction between FGFR1 and NCAM and evidence for a regulatory role of ATP, *Structure* **11**, 691–701.
30. Li, L. H., Milner, L. A., Deng, Y., Iwata, M., Banta, A., Graf, L., Marcovina, S., Friedman, C., Trask, B. J., Hood, L., and Torok-Storb, B. (1998) The human homolog of rat Jagged1 expressed by marrow stroma inhibits differentiation of 32D cells through interaction with Notch1, *Immunity* **8**, 43–55.
31. Saito, A., Suzuki, Y., Ogata, S., Ohtsuki, C., and Tanihara, M. (2004) Prolonged ectopic calcification induced by BMP-2-derived synthetic peptide, *J. Biomed. Mater. Res., Part A* **70A**, 115–121.
32. Kiessling, L. L., Gestwicki, J. E., and Strong, L. E. (2006) Synthetic multivalent ligands as probes of signal transduction, *Angew. Chem., Int. Ed.* **45**, 2348–2368.
33. Amit, M., Carpenter, M. K., Inokuma, M. S., Chiu, C. P., Harris, C. P., Waknitz, M. A., Itskovitz-Eldor, J., and Thomson, J. A. (2000) Clonally derived human embryonic stem cell lines maintain pluripotency and proliferative potential for prolonged periods of culture, *Dev. Biol.* **227**, 271–278.
34. Pyle, A. D., Lock, L. F., and Donovan, P. J. (2006) Neurotrophins mediate human embryonic stem cell survival, *Nat. Biotechnol.* **24**, 344–350.
35. Omer, B. P., Derda, R., Lewis, R. L., Thomson, J. A., and Kiessling, L. L. (2004) Arrays for the combinatorial exploration of cell adhesion, *J. Am. Chem. Soc.* **126**, 10808–10809.
36. Chaudhury, M. K., and Whitesides, G. M. (1992) How to make water run uphill, *Science* **256**, 1539–1541.
37. Stenger, D. A., Georger, J. H., Dulcey, C. S., Hickman, J. J., Rudolph, A. S., Nielsen, T. B., McCort, S. M., and Calvert, J. M. (1992) Coplanar molecular assemblies of aminoalkylsilane and perfluorinated alkylsilane—characterization and geometric definition of mammalian-cell adhesion and growth, *J. Am. Chem. Soc.* **114**, 8435–8442.
38. Kleinfeld, D., Kahler, K. H., and Hockberger, P. E. (1988) Controlled outgrowth of dissociated neurons on patterned substrates, *J. Neurosci.* **8**, 4098–4120.
39. Liesi, P., Narvanen, A., Soos, J., Sariola, H., and Snounou, G. (1989) Identification of a neurite outgrowth-promoting domain of laminin using synthetic peptides, *FEBS Lett.* **244**, 141–148.
40. Schense, J. C., Bloch, J., Aebischer, P., and Hubbell, J. A. (2000) Enzymatic incorporation of bioactive peptides into fibrin matrices enhances neurite extension, *Nat. Biotechnol.* **18**, 415–419.
41. Li, Y. J., Chung, E. H., Rodriguez, R. T., Firpo, M. T., and Healy, K. E. (2006) Hydrogels as artificial matrices for human embryonic stem cell self-renewal, *J. Biomed. Mater. Res., Part A* **79A**, 1–5.
42. Hubbell, J. A. (1999) Bioactive biomaterials, *Curr. Opin. Biotechnol.* **10**, 123–129.
43. Engler, A. J., Sen, S., Sweeney, H. L., and Discher, D. E. (2006) Matrix elasticity directs stem cell lineage specification, *Cell* **126**, 677–689.
44. Mohr, J. C., de Pablo, J. J., and Palecek, S. P. (2006) 3-D microwell culture of human embryonic stem cells, *Biomaterials* **27**, 6032–6042.
45. Metallo, C. M., Mohr, J. C., Detzel, C. J., de Pablo, J. J., Van Wie, B. J., and Palecek, S. P. (2007) Engineering the stem cell microenvironment, *Biotechnol. Prog.* **23**, 18–23.
46. Chai, C., and Leong, K. W. (2007) Biomaterials approach to expand and direct differentiation of stem cells, *Mol. Ther.* **15**, 467–480.
47. Cukierman, E., Pankov, R., Stevens, D. R., and Yamada, K. M. (2001) Taking cell-matrix adhesions to the third dimension, *Science* **294**, 1708–1712.
48. Cukierman, E., Pankov, R., and Yamada, K. M. (2002) Cell interactions with three-dimensional matrices, *Curr. Opin. Cell Biol.* **14**, 633–639.
49. Flemming, R. G., Murphy, C. J., Abrams, G. A., Goodman, S. L., and Nealey, P. F. (1999) Effects of synthetic micro- and nano-structured surfaces on cell behavior, *Biomaterials* **20**, 573–588.
50. Hartgerink, J. D., Beniash, E., and Stupp, S. I. (2002) Peptide-amphiphile nanofibers: A versatile scaffold for the preparation of self-assembling materials, *Proc. Natl. Acad. Sci. U.S.A.* **99**, 5133–5138.
51. Bain, C. D., Troughton, E. B., Tao, Y. T., Evall, J., Whitesides, G. M., and Nuzzo, R. G. (1989) Formation of monolayer films by the spontaneous assembly of organic thiols from solution onto gold, *J. Am. Chem. Soc.* **111**, 321–335.
52. Silva, G. A., Czeisler, C., Niece, K. L., Beniash, E., Harrington, D. A., Kessler, J. A., and Stupp, S. I. (2004) Selective differentiation of neural progenitor cells by high-epitope density nanofibers, *Science* **303**, 1352–1355.
53. Houseman, B. T., and Mrksich, M. (1998) Efficient solid-phase synthesis of peptide-substituted alkanethiols for the preparation of substrates that support the adhesion of cells, *J. Org. Chem.* **63**, 7552–7555.
54. Luk, Y. Y., Kato, M., and Mrksich, M. (2000) Self-assembled monolayers of alkanethiolates presenting mannitol groups are inert to protein adsorption and cell attachment, *Langmuir* **16**, 9604–9608.